LOCAL IONOSPHERIC MODELLING OF GPS CODE AND CARRIER PHASE OBSERVATIONS

H. Nahavandchi and A. Soltanpour

Norwegian University of Science and Technology, Division of Geomatics,
Trondheim, Norway

ABSTRACT

A limiting factor for successful ambiguity resolution in precise GPS positioning is the existence of un-modelled ionospheric errors in both the carrier phase and the pseudorange measurements. In this study, the ionospheric delay is modelled using a four-parameter polynomial utilizing dual frequency observations in the region of study in southern Iran. Thereafter, the corrected and non-corrected observations for ionospheric delay are compared with the ionospheric-free solution of the same observations. Two baselines (15 km and 72 km) are used for this comparison. An improvement of 0.22 ppm and 0.07 ppm is achieved, respectively, for the two baselines. Further, the ionospheric delay is modelled using two other methods, i.e. the Klobuchar and divergence models. The divergence model uses single frequency observations. The improvement of the results is restricted as the noise level in code observations is high. An improvement of 0.15 ppm for the 72 km baseline and no improvement for the 15 km baseline are observed using the divergence model. The Klobuchar model corrects 50%-60% of the ionospheric errors in this study.

INTRODUCTION

GPS measurements are contaminated by several kinds of error. These error sources may be classified as satellite-dependent errors, medium-dependent errors and receiver-dependent errors. The satellite-dependent errors include the orbital errors and the satellite clock errors. The medium-dependent errors include the ionospheric and tropospheric delays. The receiver-dependent errors include the receiver noise, the receiver clock error, the multipath error and the antenna phase-centre variations. Some of these errors can be eliminated or reduced through differencing between the satellites or between the receivers.

The ionosphere is a layer of the atmosphere in which the GPS signal propagation is dependent on the density of the electrons and the frequency of the signal. The ionospheric effect on GPS observations, expressed as phase advance and code delay, changes from one metre to above one hundred metres in high solar activity periods and certain other circumstances. The relative error due to the ionospheric effect may reach a few ppm. Using dual frequency receivers is the best way for correcting this error. Ionospheric Total Electron Content (TEC) predictions are also used for ionospheric modelling (e.g. [**12**]). Also, some methods have been implemented when dual frequency observations are not available (e.g. [**7**], [**11**]).

GPS carrier phase observations are used for precise relative positioning. In this way only the difference in the ionospheric delay observed at two stations is of importance. Since ionospheric parametres are spatially correlated, the broad features of dispersive delay observed in each of two stations disappear. The ionospheric propagation effects in geodetic GPS positioning have been investigated and computed by many researchers (e.g. [**1**], [**6**], [**4**], [**11**], [**2**], [**10**]). Some correction methods for GPS ionospheric error are listed in [**8**].

Different models have been suggested for modelling the ionospheric effect. However, because of the complexity of the ionosphere and its changes with time and location, the models might not be effective enough. In this study, a four-parameter local model has been investigated, which uses the dual frequency data available in the

study region. Other models have also been investigated and compared with the four-parameter model.

IONOSPHERIC ERROR MODELLING

The ionosphere is generally considered to be the part of the atmosphere from approximately 50 to 1000 km altitude in which a fraction of the gas molecules have been ionized by ultra-violet radiation from the Sun ([**3**]). There are different models to handle the ionospheric effects in GPS positioning. Some of them were studied in this paper. Finding an appropriate local model for the ionosphere delay is difficult. The use of dual frequency observations is the best procedure to correct the ionospheric effects and is chosen here to evaluate the performance of the tested models.

Klobuchar Model

This model uses the ionospheric coefficients broadcast by GPS satellites. First, the effect will be estimated in the vertical direction above the observation station; thereafter, it will be mapped to the satellite-receiver path. A cosine form is used to approximate the vertical ionospheric delay d_{ion}^{v}. This effect reaches its maximum value at 14:00 hours local time. The model for the vertical ionospheric time delay (in time unit) can be written ([**7**], [**5**]):

$$d_{ion}^{v} = A_1 + A_2 + \cos\left(\frac{2\pi(t - A_3)}{A_4}\right) \tag{1}$$

where

$$\begin{aligned} A_1 &= 5\times10^{-9} \text{ (seconds)} \\ A_2 &= \alpha_1 + \alpha_2\varphi_{IP}^{m} + \alpha_3\varphi_{IP}^{m\,2} + \alpha_2\varphi_{IP}^{m\,3} \\ A_3 &= 14 \text{ (local time in hours)} \\ A_4 &= \beta_1 + \beta_2\varphi_{IP}^{m} + \beta_3\varphi_{IP}^{m\,2} + \beta_2\varphi_{IP}^{m\,3} \end{aligned} \tag{2}$$

where A_1 and A_3 are constant and the coefficients α and β are broadcast by the satellites. The parameter t is the local time of the ionospheric intercept point (IP) (the ionospheric point is the intersection of the ionospheric layer and the satellite signal in the mean ionospheric height) and can be computed from:

$$t = \frac{\lambda_{IP}}{15} + t_{ut} \tag{3}$$

where λ_{IP} is the longitude of the ionospheric intercept point and t_{ut} is the UT time of the observation. The spherical latitude of the ionospheric point φ_{IP}^{m} can be computed from:

$$\cos\varphi_{IP}^{m} = \sin\varphi_{IP}\sin\varphi_P + \cos\varphi_{IP}\cos\varphi_P\cos(\lambda_{IP} - \lambda_P) \tag{4}$$

where the latitude and longitude of the magnetic pole (P) are:

$$\begin{aligned} \varphi_P &= 73.8^{\circ} \\ \lambda_P &= 291.0^{\circ} \end{aligned} \tag{5}$$

Finally the ionospheric delay in the signal path can be computed from:

$$d_{ion} = \frac{1}{\cos Z'} d_{ion}^{v} \tag{6}$$

where the zenith angle, *Z'*, of the satellite at ionospheric point can be computed from:

$$\sin Z' = \frac{R}{R + h_m} \sin Z \tag{7}$$

where R is the mean Earth radius and h_m is the mean height of the ionospheric point. The coordinates of the ionospheric point (φ_{IP} , λ_{IP}) can be computed from the elevation (E) and azimuth (AZ) of the satellite and the approximate coordinates of the observation station (φ, λ):

$$\begin{aligned} \varphi_{IP} &= \arcsin\left(\cos\varphi \cos E + \cos\varphi \sin E \cos AZ\right) \\ \lambda_{IP} &= \lambda + \arcsin\left(\frac{\sin E \sin AZ}{\cos\varphi}\right) \end{aligned} \tag{8}$$

The mean height h_m of the ionospheric point is generally chosen between 300 and 400 km. It has been shown that the Klobuchar Model reduces the ionospheric error by 50% to 60% (see e.g. [**8**]).

Divergence Model

The code-carrier phase divergence property of the ionosphere at GPS frequencies is used to derive the group delay, or, alternatively, the carrier phase advance, using single frequency observations ([**7**]). In this method, the pseudorange and carrier phase observations from the carrier frequency L1 are used. For best results, the multipath effect should be at a minimum.

The carrier phase Φ and pseudorange measurements P can be expressed as follows:

$$P_1 = \rho + c(dt - dT) + d_{ion_1} + d_{trop} + mp_{P_1} + noise_{P_1} \tag{9}$$

$$\Phi_1 = \rho + c(dt - dT) + \lambda_1 N_1 - d_{ion_1} + d_{trop} + mp_{\Phi_1} + noise_{\Phi_1} \tag{10}$$

where Φ is the observed carrier phase multiplied by the carrier wavelength $\boldsymbol{\lambda}$, P is the measured pseudorange, ρ is the geometric range between the receiver and the GPS satellite, the subscript *(1)* denotes the L_1 frequency, c is the speed of light, dt and dT are the offsets of the satellite and receiver clocks from the GPS time, N is the initial integer ambiguity parameter, d_{ion} and d_{trop} are the ionospheric and tropospheric delays, mp_Φ and mp_P are the carrier phase and the pseudorange multipath errors (assumed to be zero), $noise_\Phi$ and $noise_P$ represent the system noise in the carrier phase and the pseudorange measurements, respectively.

The divergence method uses the difference between the pseudorange and carrier phase observations in equations (9) and (10) and finally, after some mathematical simplifications, arrives at the following formula for the ionospheric delay ([**11**]):

$$d_{ion_1} = 0.5(P_1 - \Phi_1 + \lambda_1 N_1) \tag{11}$$

The key problem in the equation (11) is to separate the integer ambiguity from the ionospheric delay. To do this, an obliquity function is introduced to map the vertical

delay at the ionospheric intercept point to the line-of-sight delay at the user location. The obliquity function O(E) can be expressed in terms of the satellite elevation angle E (=90º-Z) ([**6**]):

$$O(E) = 1 + 2\left(\frac{96 - E}{90}\right)^3 \tag{12}$$

In the next step the vertical group delay is divided to two parts: a standard ionospheric correction I_s and a residual vertical delay I_v ([**11**]):

$$P_1 - \Phi_1 - 2I_s O(E) = 2I_v O(E) - \lambda_1 N_1 \tag{13}$$

The standard ionospheric correction can be computed from the Klobuchar model. The residual vertical delay is a function of satellite elevation and azimuth, time and the user location. If it could be assumed that the vertical TEC remains constant in the observation period, one can express the vertical residual delay from a third order polynomial as ([**11**]):

$$\begin{aligned} I_v = {} & a_{00} + a_{10}\varphi_{IP} + a_{11}\lambda_{IP} + a_{20}\varphi_{IP}^2 + a_{21}\varphi_{IP}\lambda_{IP} + a_{22}\lambda_{IP}^2 + \\ & a_{30}\varphi_{IP}^3 + a_{31}\varphi_{IP}^2\lambda_{IP} + a_{32}\varphi_{IP}\lambda_{IP}^2 + a_{33}\lambda_{IP}^2 \end{aligned} \tag{14}$$

Substitution of equation (14) into equation (13) provides an observation equation in which the ten coefficients *a* along with the ambiguity in phase *N* can be computed using a least-squares procedure over the observation period. Thereafter, the absolute group delay in the trajectory to the satellite can be estimated as $d_{ion_1} = (I_s + I_v)O(E)$.

The Four-Parameter Model

It is a common procedure in processing carrier phase observations to use the double differences (*DD*) to eliminate a number of common errors. Equation (10) in double difference mode can be written as:

$$DD\Phi = DD\rho + \lambda DDN - DDd_{ion} + DDd_{trop} + DDmp_{\Phi} + noise_{DD} \tag{15}$$

In the next step, equation (10) for the carrier signal L2 is subtracted from the observation equation for the carrier signal L1 (again assuming negligible multipath errors):

$$\Phi_1 - \Phi_2 = \lambda_1 N_1 - \lambda_2 N_2 + d_{ion2} - d_{ion_1} + noise_{\Phi_1 - \Phi_2} \tag{16}$$

Using (see e.g. [**13**])

$$d_{ion} = -c\frac{40.3TEC}{f^2} + o\left(\frac{1}{f^3}\right) \tag{17}$$

where *f* is the frequency of the signal and neglecting the term $o\left(\frac{1}{f^3}\right)$, one obtains:

$$F(\Phi_1 - \Phi_2) = F(\lambda_1 N_1 - \lambda_2 N_2) - d_{ion_1} + noise_{\Phi_1 - \Phi_2} \tag{18}$$

where

$$F = \frac{f_2^2}{f_2^2 - f_1^2} \tag{19}$$

and f_1 and f_2 are the frequencies of the carrier signals L1 and L2. Equation (18) can now be written in double difference form for two satellites and two receivers. One gets the double difference of the ionospheric phase delay:

$$F(DD\Phi_1 - DD\Phi_2) = F(\lambda_1 DDN_1 - \lambda_2 DDN_2) - DDd_{ion_1} + DDnoise_{\Phi_1-\Phi_2} \tag{20}$$

Equation (20) contains a double difference ionospheric delay and a constant term assuming no cycle slips. It should be mentioned that the constant part of the ionospheric term will be absorbed by the phase ambiguity in the computation processes. Any non-constant part not absorbed by parameters can affect the estimation and will show up in the residuals of the adjustment procedure. On the other hand, equation (20) can be used in equation (15) to get the double difference ionosphere free carrier phase observations (after some mathematical simplifications, see also [**9**]):

$$G(DD\Phi_1 - DD\Phi_2) = DD\rho + G(\frac{DDN_1}{\lambda_1} - \frac{DDN_2}{\lambda_2}) + DDd_{trop} + noise_{tot} \tag{21}$$

where

$$G = \lambda_2^2 F \tag{22}$$

It is obvious that this combination of the carrier phase observations is free from ionospheric delay. However, the combination of different observations raises the noise level considerably.

The double frequency observations can be used to determine a local ionospheric model. The dependency of the ionospheric delay on the frequency of the carrier signals enables us to remove this delay using double frequency observations. Using equations (18) and (6) one can write:

$$F(\Phi_1 - \Phi_2) = -\frac{d^v_{ion_1}}{\cos Z'} + k + noise_{\Phi_1-\Phi_2} \tag{23}$$

where k is a constant term including the ambiguity in the phases of the carrier signals L1 and L2. Further, a polynomial model can be considered for the vertical ionospheric delay as a function of latitude and hour angle of the Sun referred to the ionospheric intercept point. The hour angle h of the Sun is the angle between the astronomical meridian of the Sun and that of the observer. This model is of the first order for the latitude and second order for the hour angle for the observations up to 5 hours in duration ([**9**]):

$$d^v_{ion_1} = a_0 + a_1\varphi_{IP} + a_2 h + a_3 h^2 \tag{24}$$

Putting this polynomial in equation (23) for all satellites observed and for all epochs, one arrives in an over-determined equation system with 4 unknown coefficients a and n constant unknowns k for n satellites. The $-1/\cos Z'$ term in equation (23) guarantees the separation of the ionospheric delay from the ambiguity in phase. It should be noted that cycle slips should be removed or solved prior to these

computations to ensure enough degrees of freedom. The advantage of this model is the use of only carrier phase observations, which makes it more accurate than models using code observations.

EXPERIMENTAL TESTING OF MODELS

To model the ionospheric effect locally, three stations (see Figure 1) were observed using double frequency Trimble 4000SSI GPS receivers with chokering antennas to reduce the multipath effects. Site selection also aimed at reducing multipath. Where needed (for baseline solutions and point positioning) the data collected were processed with Trimble GPSurvey software with ambiguities fixed to their integer values. Otherwise, a PC program was developed for further numerical investigations. Depending on the tested ionospheric model, other solutions were also applied (see experimental testing of each model). Among them were the double frequency ionospheric-free solution and the single difference solution. The ionospheric-free solution was used for the comparison of the accuracy of the ionospheric models. The three stations JASK, 1637 and 1532 were chosen to give a short (15 km) and a long (72 km) baseline for analysis of the ionospheric errors. The baseline JASK-1637 was 72 km long and was observed over two hours with a recording rate of 10 s. The baseline 1637-1532 was 15 km long and was observed over 25 minutes with a recording rate of 10 s. The short observation time on the shorter baseline was intentional to investigate the modelling efficiency of both short and long observation time. The data sets used in this study were measured on 17 December 1998. The average temperature was 25° with a middle humidity (50%). It should be noted that larger values for the ionospheric delays are expected during periods of maximum solar activity. At the end of 1999 and at the beginning of 2000, the solar activity reached its maximum. Figure 1 shows the locations of the three sites JASK, 1637 and 1532.

The cycle slips were removed from the observations prior to the computations. The tropospheric model of Saastamoinen and the IGS precise ephemerides were used for the computations. Although this study put no emphasis on the process of estimating the ambiguity term, the importance of using a valid estimate of the integer ambiguity should be noted. For all baseline solutions, the ambiguities were successfully fixed to integer values except for the long baseline in the case where no ionospheric model was applied (see Table 3).

In the next step, the ionospheric error for station JASK and satellite SV19 was computed using equation (18). The results are shown in Figure 2, together with the elevation and azimuth of the satellite. It can be seen that the ionospheric error decreased with an increase in the elevation of the satellite. The maximum value of the ionospheric errors was 0.63 m when SV19 was at its lowest elevation. It should be noted that the ionospheric errors are computed for all available satellites in the observation period, however, the results of some selected satellites are shown.

Using equation (20) the ionospheric effect in the double difference case was computed for the baseline JASK-1637 (72 km) and is shown in Figure 3 for satellites SV2, SV19, and SV27. Satellite SV13 was chosen as the reference satellite. The absolute maximum value of the ionospheric error was 0.15 m for SV2 and the minimum value of the ionspheric error was 0.075 m for SV27.

The single difference solution [writing equation (18) in single difference form for one satellite and two receivers] was used for the baseline 1637-1532 (15 km) for the same satellites, as the observation time for this baseline was short. The results of this solution are depicted in Figure 4. The smaller relative ionospheric delay was obtained because the baseline was shorter. Further, the residuals of the double difference carrier

phase observations for the least-squares adjustment of both baselines were computed and the results are shown in Table 1. Since all other error sources were essentially minimised the residuals show only the influence of un-modelled residual ionospheric errors. The results of Table 1 are comparable with the ionspheric delays shown in Figures 3 and 4.

Next, the differences from single frequency and double frequency solutions for different baselines were examined. To do this, 10 baselines (7-105 km) were measured and processed using the ionospheric-free double frequency observable [see equation (21)]. The two baselines discussed above were part of the analysis. Single-frequency solutions without any ionospheric modelling were also computed. All baselines were in the same geographical area as shown in Figure 1. The observation times for all baselines were 2 hours. Figure 5 shows the baseline length errors due to un-modelled ionospheric delays. The differences reach 110 mm. As expected, the ionospheric effects are larger for long baselines.

Ionospheric Effect Modelling

Klobuchar and Four-Parameter Models

In a first step, the four-parameter model of equation (24) was used to compute the vertical ionospheric delay in the region around station JASK. The geographic region for these computations extends 35° in longitudes and 30° in latitude. Station JASK is in the middle of this selected region. The ionospheric intercept point elevation was chosen to be 350 km and the zenith angle of the signal path, the coordinates of the ionospheric point and the hour angle of the Sun were computed using the broadcast ephemeris and the approximate coordinates of the receiver. The local time is 13:30. Figure 6 shows the result of these computations for the vertical ionospheric delay. The maximum value reaches to 5.64 m in low latitudes. Vertical delay varies more than 1 m. It should be noted that Figure 6 presents the ionospheric vertical delay. Using equation (6) the ionospheric delay in the signal path can be computed. These results of the four parameter model in the large region around JASK station [after using equation (6)] are comparable with those shown in Figure 7 (see below).

For the comparison, the ionospheric effects computed using the four-parameter model are plotted in Figure 7 together with the delays computed from the Klobuchar model [equation (1)] and the double-frequency solution [see equation (18)]. Station 1637 and SV13, SV18 and SV27 are chosen for these computations. The ionospheric effects range from 5 to 11 m. Figure 7 shows that the four-parameter model agreed best with the double frequency solution while the Klobuchar model agreed with the double frequency solution only to a few metres. The four-parameter model was used for the correction of the ionospheric error in the L1 code and carrier phase observations. The model was computed using observations at station JASK which was then applied to the two other stations. The ionospheric-free solution was used as the "true solution" for comparison. Table 2 shows the results before and after the model was used for the two baselines. The advantages of using the four-parameter model to fix ambiguities and to improve the accuracy of the baseline solutions are obvious from Table 2. An improvement of 0.22 ppm for the 72 km baseline was observed. The differences between the ionospheric delay computed from the four-parameter model and the double frequency solutions are plotted in Figure 8. These differences varied between 2 and 10 cm. The four-parameter model was also applied to the other 8 baselines in the test area. Improvements in the accuracy of the solutions in a comparison with ionospheric-free solution were at a similar level to those reported above, with the level of improvement increasing with baseline length.

Divergence Model

Equation (11) was used to compute the ionospheric effect with the divergence model on the L1 signal. Stations JASK and 1532 were used. Figures 9 and 10 show the ionospheric effects. Comparison of Figure 2 with Figures 9 and 10 shows the efficiency of the divergence model to correct for the ionospheric errors, but the presence of the noise in C/A code pseudorange is observed in the divergence model (see Figures 9 and 10). Therefore one can expect better accuracies with the four-parameter model than the divergence model. The differences between the divergence model and the double frequency solution in estimating the ionospheric effect are shown in Figures 11 and 12 for stations JASK and 1532, respectively. The maximum differences of 0.45 m at JASK and 2.21 m at 1532 are observed. The large difference of ionospheric error estimation for station 1532 was likely caused by the high noise level of code observations as well as the shorter observation time.

Next, the ionospheric error computed for stations JASK, 1637, and 1532 was used in the L1 code and carrier phase observation computations as a correction term. The results before and after the use of the model are summarized in Table 3. Improvements are observed in the baseline JASK-1637, but not in the baseline 1637-1532. As mentioned before, the high noise level and a short observation time were the likely reason for the poorer result on the baseline to 1532.

GENERAL REMARKS AND CONCLUSIONS

Local ionospheric modelling is an important tool for improving the accuracy of positioning for single frequency GPS users because the ionospheric delay is the largest error source in GPS since Selective Availability (SA) was turned off in May 2000. In this paper different models were studied and tested to estimate the ionospheric effects. The comparison of the accuracy of the different modelling attempts was made against the ionospheric-free double frequency solution.

The four-parameter model reduced the ionospheric errors significantly. This model used double-frequency data available in the region for definition of a local model. The use of more than one station (with double frequency data) and longer observation time for the local model definition must be studied. Permanent GPS stations can be very useful to define a local ionospheric model. The use of a better analytical model enables better accuracy to be achieved for the vertical ionospheric delay estimation. In this regard one can use a coordinate system oriented to the Sun or use a polynomial with higher orders.

The divergence model was also investigated for its ability to estimate the ionospheric effect. This method only uses the single frequency data for the local model determination. The L1 code and carrier phase data are used. This method also reduces the ionospheric errors, significantly. However, the presence of the noise (due to the code observations) makes the estimation less accurate compared to the four-parameter model. In this model, it is critical that the ionospheric conditions be the same in the observation time period. In both models, it is important that cycle slips be removed from the observations and multipath effects be as small as possible.

The broadcast model of Klobuchar was also examined in this study for local model estimation. This model corrects 50%-60% of the ionospheric errors and so is not suitable for the precise computations.

ACKNOWLEDGEMENTS

The authors would like to thank the two unknown reviewers for their effort in providing constructive comments on an earlier version of the manuscript. Thanks also go to the editor for his comments and time. This research was supported by a grant from the National Mapping Authority of Iran (NCC). NCC is also thanked for providing data used in this study.

References

1. Bishop, G.J., Klobuchar, J.A. and Doherty, P.H., 1985. Multipath effects on the determination of absolute ionospheric time delay from GPS signals, *Radio Science*, **[20]**: 388-396.
2. Bosy, J., Figurski, M. and Wielgosz, P., 2003. A strategy for GPS data processing in a precise local network during high solar activity, *GPS Solutions* **[7]**: 120-129.
3. Davies, K., 1990. *Ionospheric radio*, IEE Electromagnetic Waves Series 31, Peter Perigrinus Ltd. London.
4. Georgiadou, Y. and Kleusberg, A., 1988. On the effect of ionospheric delay on geodetic relative GPS positioning, *Manuscripta Geodaetica* **[13]**: 1-8.
5. Hofmann-Wellenhof, B., Lichtenegger, H. and Collins, J., 1994.*Global positioning system: Theory and practice*, Springer-Verlag, Wien New York.
6. Kleusberg, A., 1986. Ionospheric propagation effects in geodetic relative GPS positioning, *Manuscripta Geodaetica* **[11]**: 256-261.
7. Klobuchar, J.A., 1987. Ionospheric time-delay algorithm for single frequency GPS users. IEEE Transactions on Aerospace and Electronic Systems, *AES* **[23]**: 325-331.
8. Klobuchar, J.A., 2001. Eye on the ionosphere: Correction methods for GPS ionospheric range delay, *GPS Solutions* **[2]**: 91-92.
9. Nahavandchi, H. and Soltanpour A., 1999. Ionospheric effect modelling for single frequency GPS users, Technical Report, Department of Surveying and Geomatics Engineering, University of Tehran. 80 pages.
10. Olynik, M., Petovello, M.G., Cannon, M.E. and Lachapelle, G., 2002. Temporal impact of selected GPS errors on point positioning, *GPS Solutions* **[6]**: 47-57.
11. Qiu, W., Lachapelle, G. and Cannon, M.E., 1995. Ionospheric effect modelling for single frequency GPS users, *Manuscripta Geodaetica* **[20]**: 96-109.
12. Liu, Z. and Gao, Y., 2004. Ionospheric TEC predictions over a local area GPS reference network, *GPS Solutions* **[8]**: 23-29.
13. Seeber, G., 1993. *Satellite Geodesy: foundations, methods, and applications*. Walter de Gruyter, Berlin-New York. 532 pages

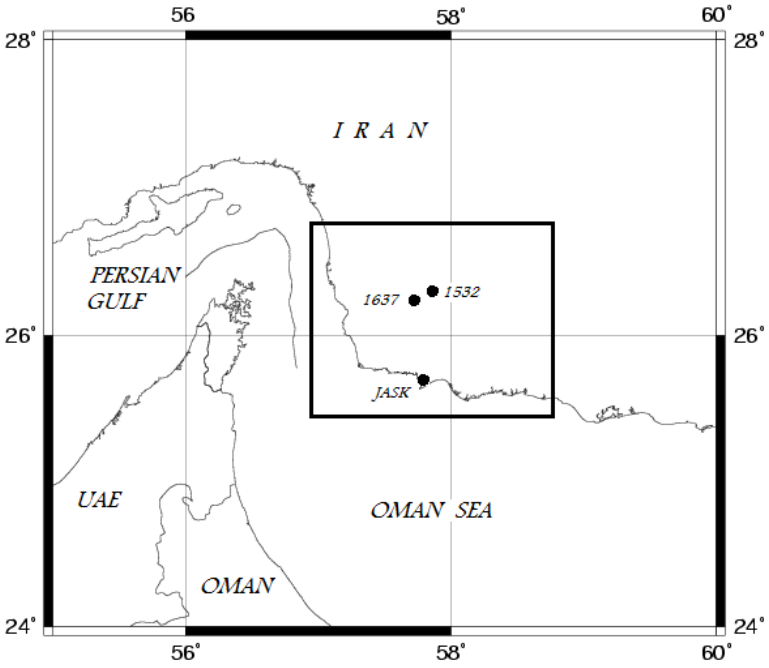

Fig.1. The location of the three sites JASK, 1637 and 1532.

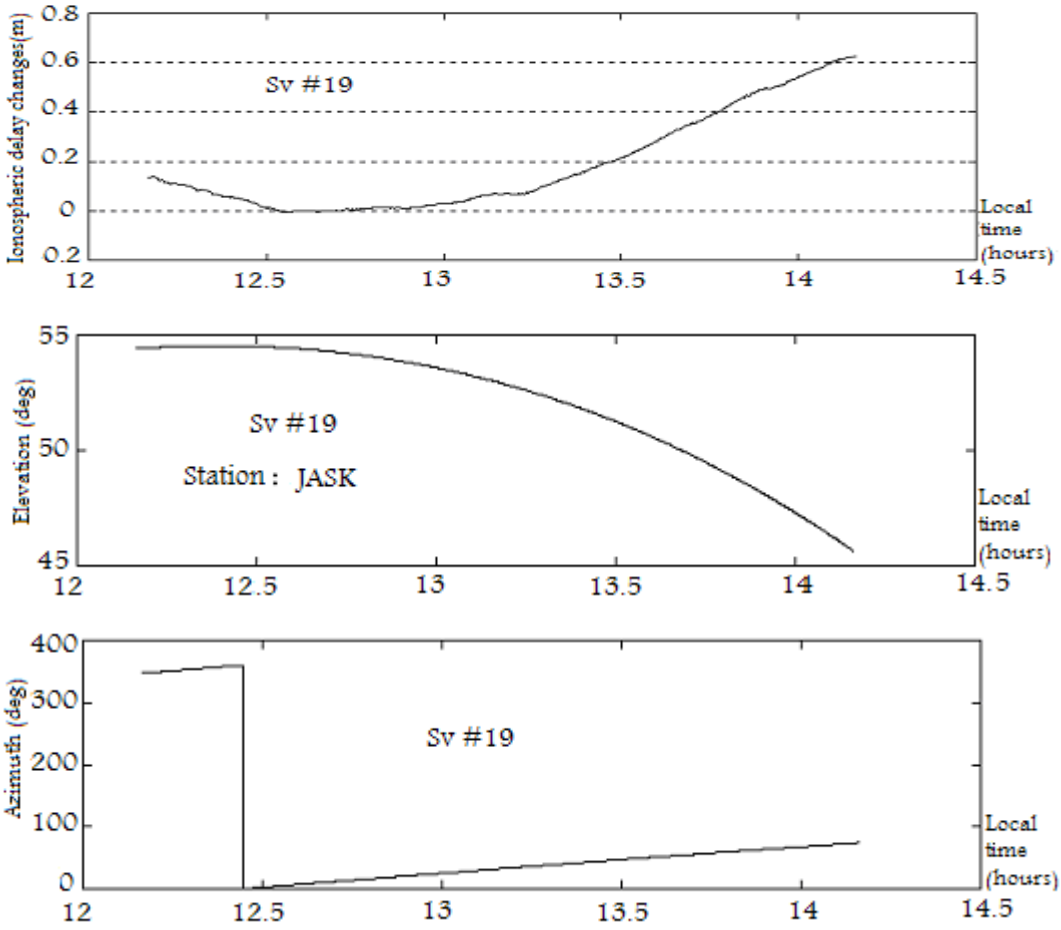

Fig.2. The ionospheric delay changes at station JASK for SV19 with the satellite's elevation and azimuth.

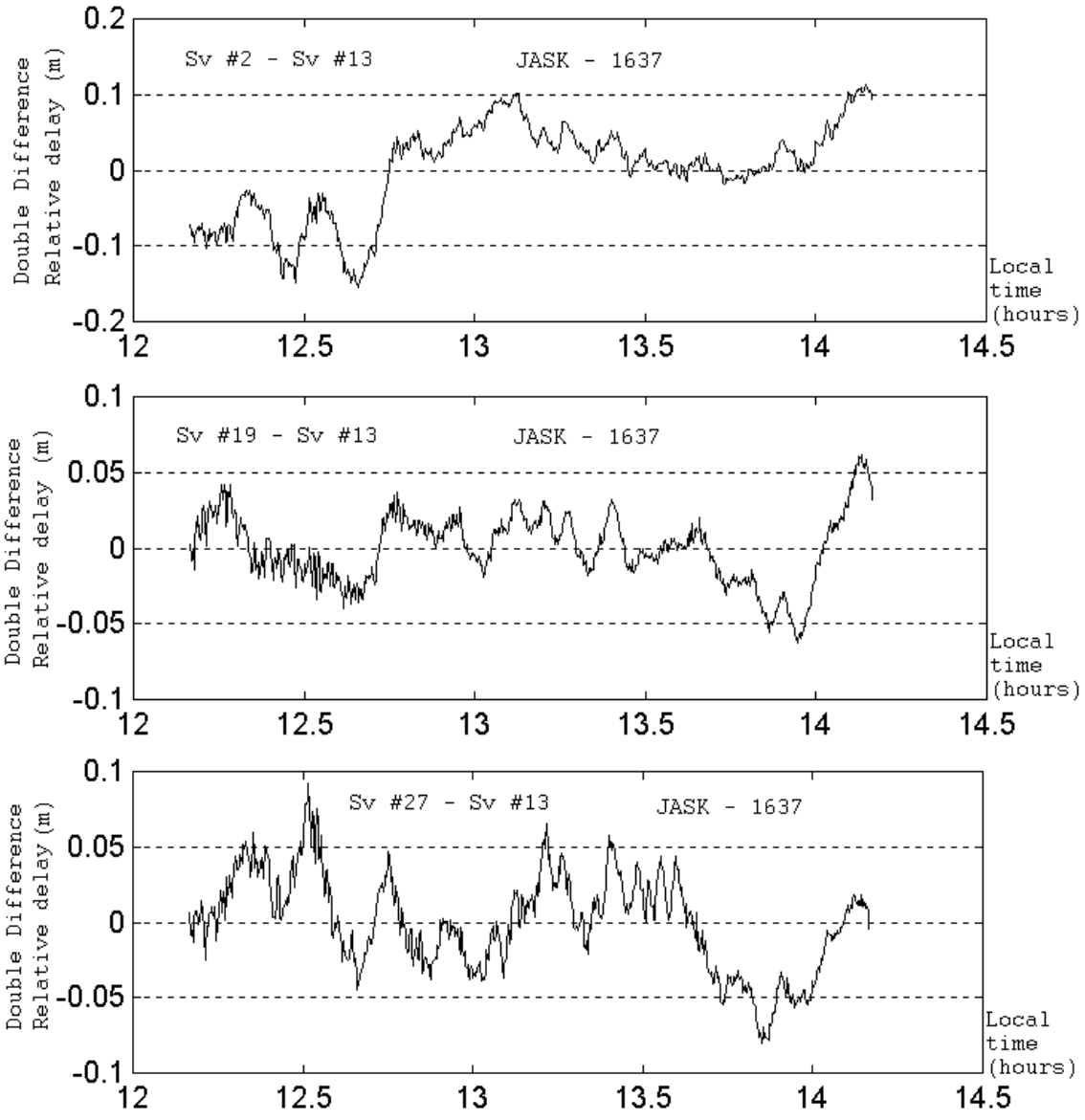

Fig.3. Double difference ionospheric delay on baseline JASK-1637 (72 km).

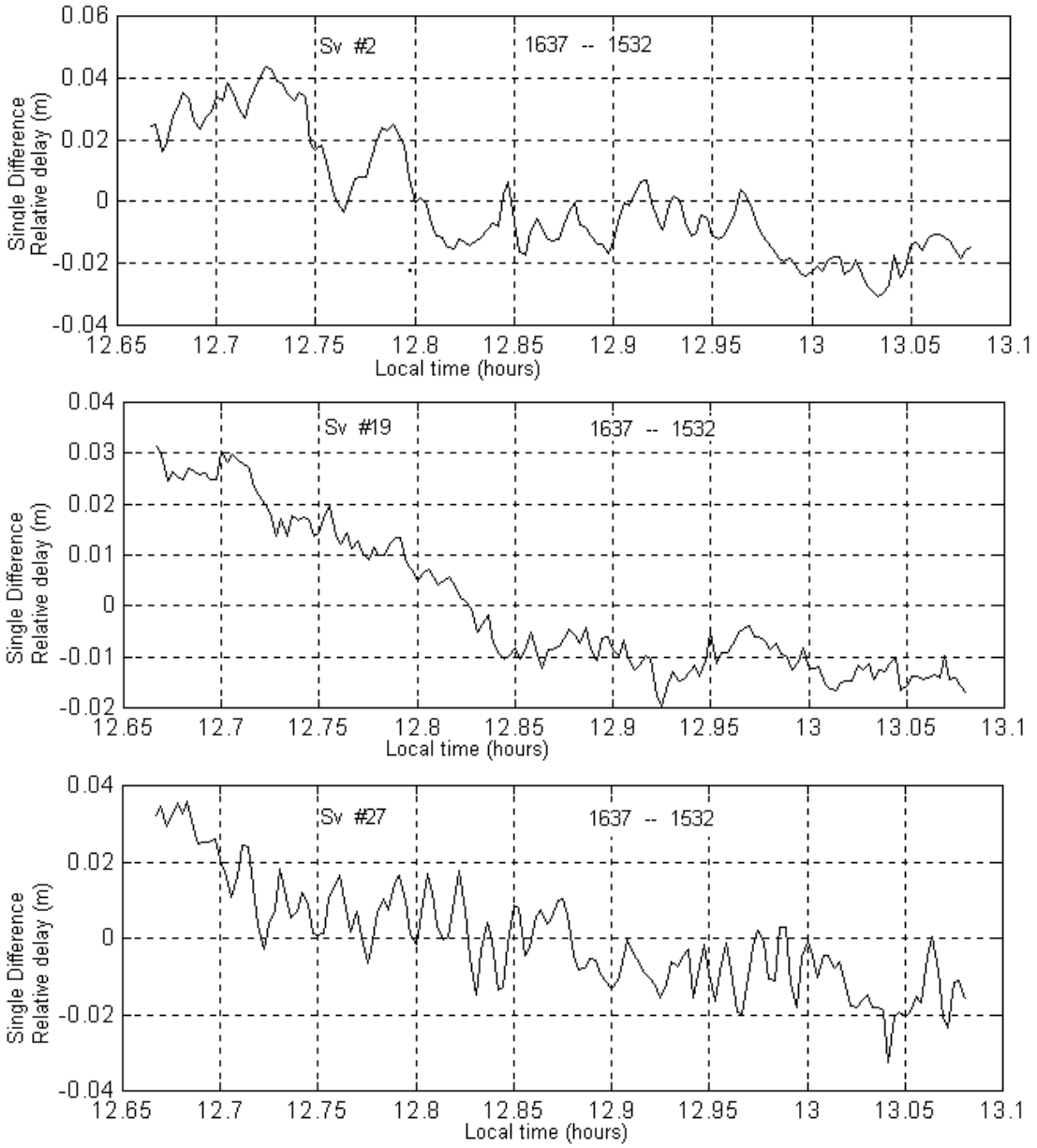

Fig.4. Single difference ionospheric delay on baseline 1637-1532.

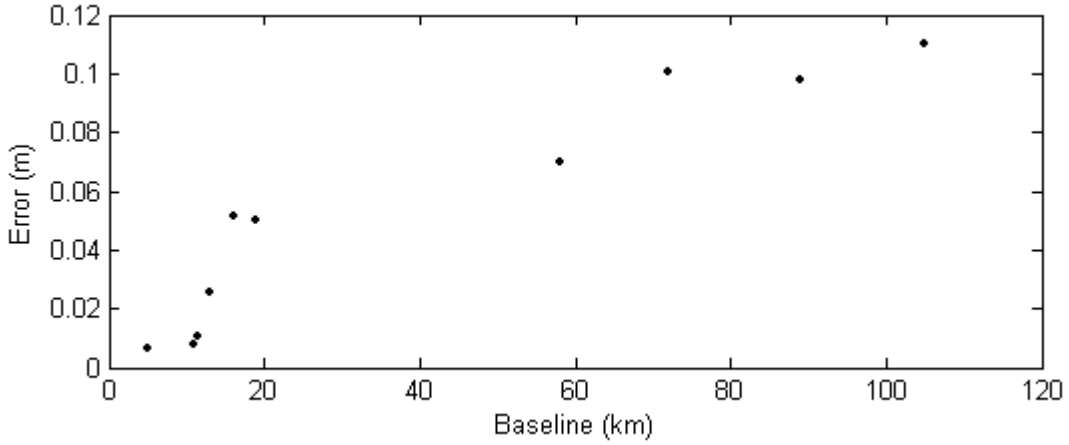

Fig.5. Baseline length error due to un-modelled ionospheric delay.

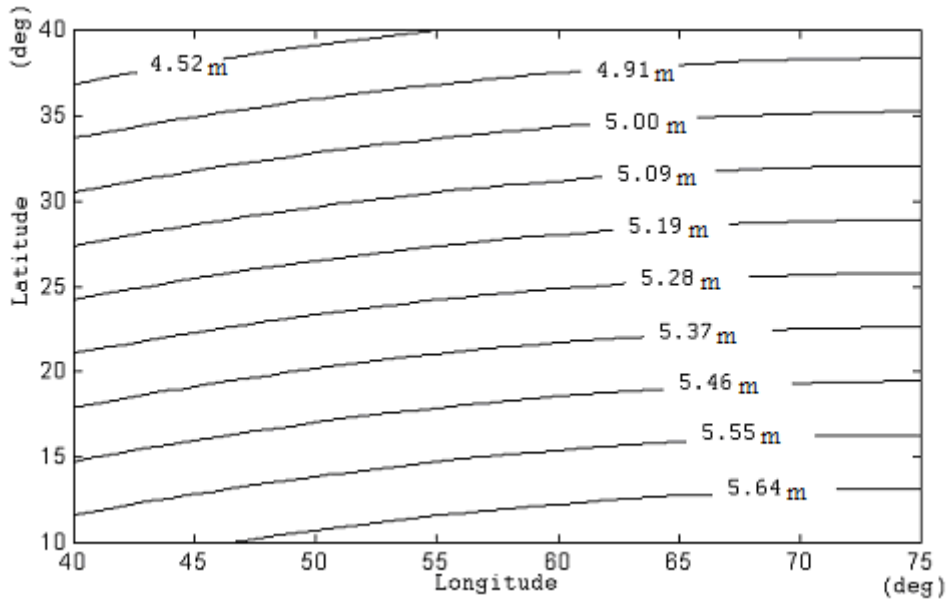

Fig.6. Vertical ionospheric delay computed from four-parameter model around JASK station in metres (13:30 local time).

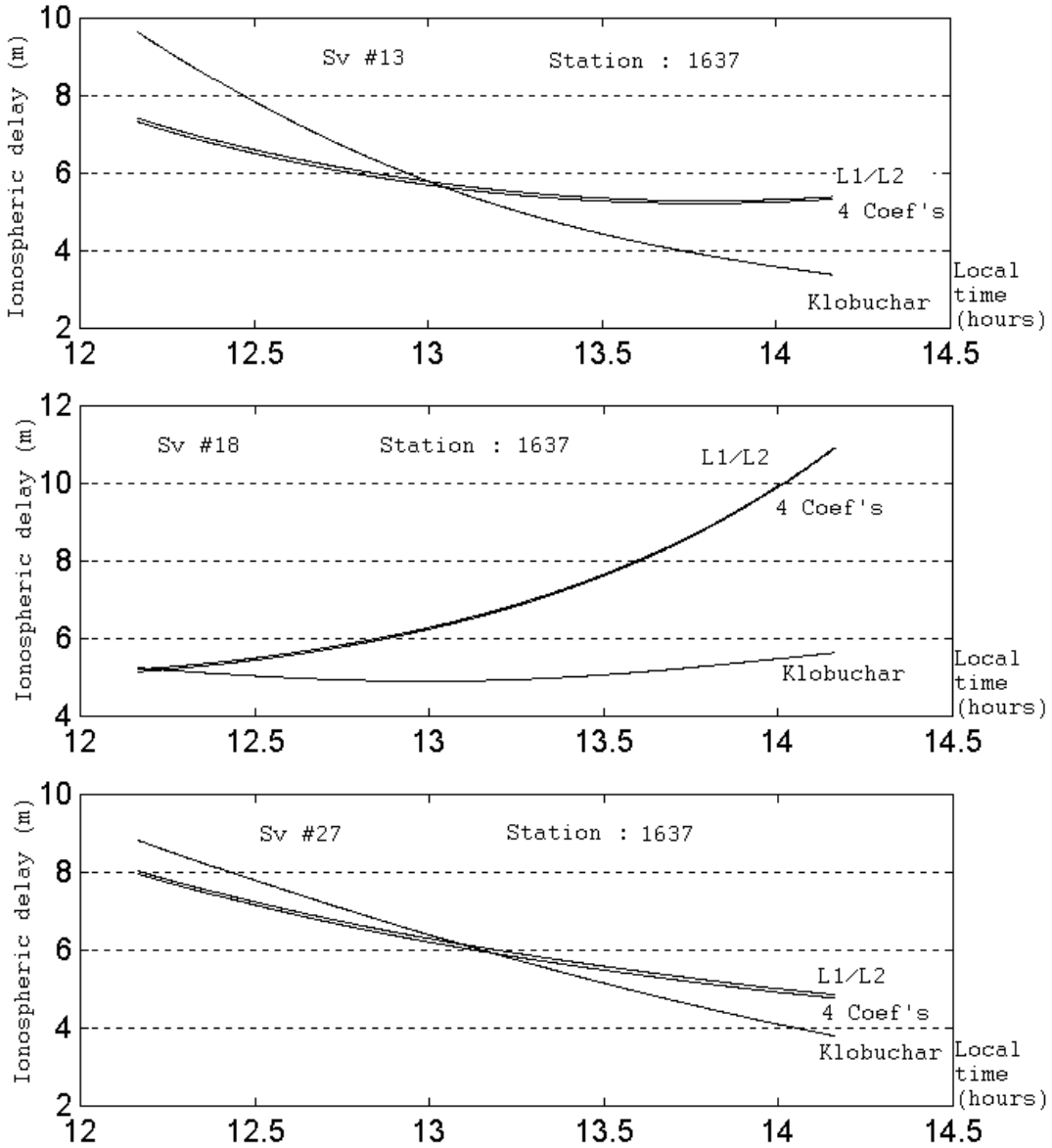

Fig.7. Ionospheric delay from satellites SV13, SV18 and SV27 at station 1637 with different models.

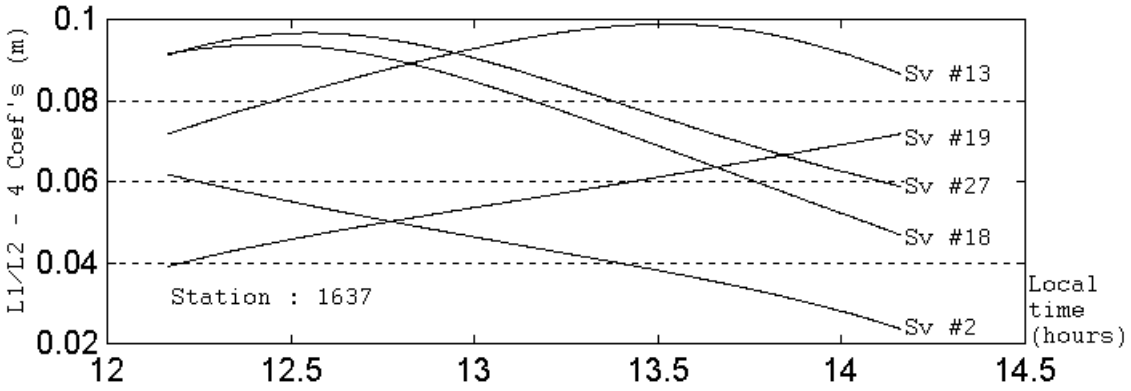

Fig.8. Differences in ionospheric delay between the four-parameter model and dual frequency solution.

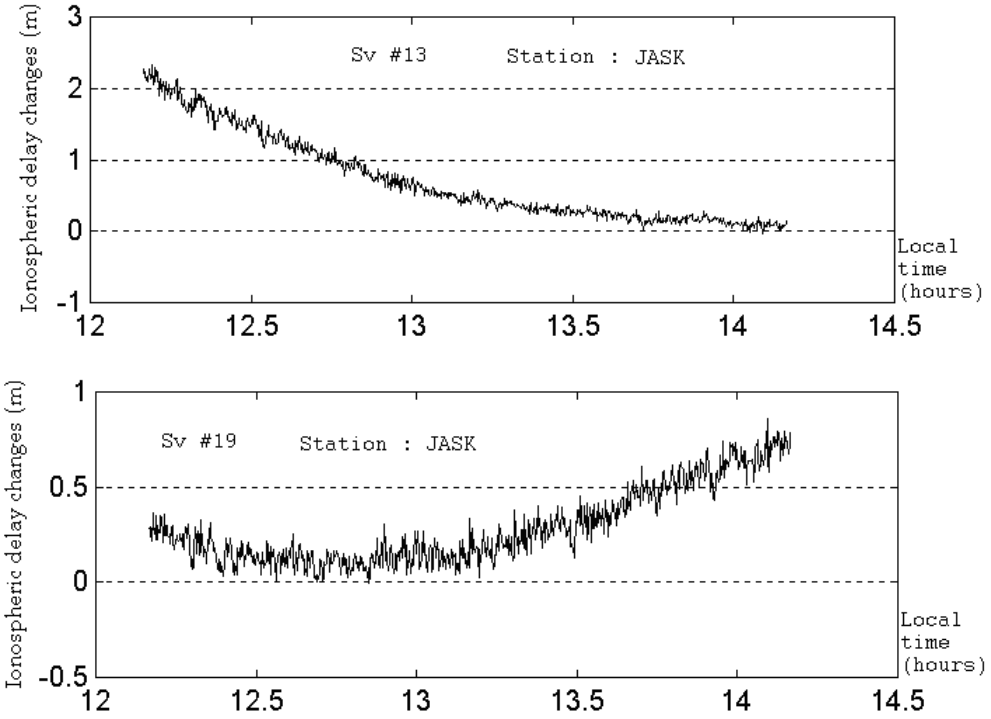

Fig.9. Relative ionospheric delay on L1 observations at station JASK computed from Divergence model.

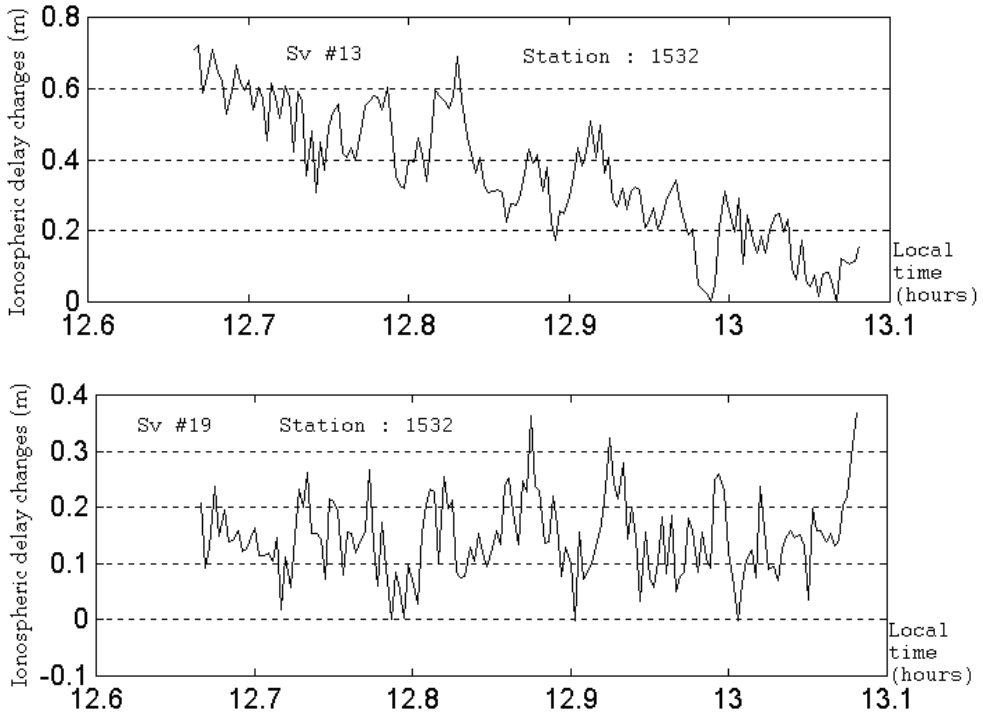

Fig.10. Relative ionospheric delay on L1 observations at station 1532 computed from Divergence model.

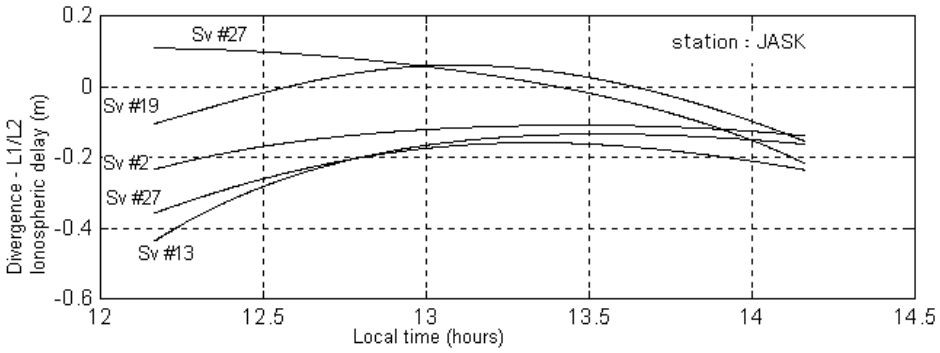

Fig.11. Differences between delays computed from divergence model and dual frequency solution at station JASK.

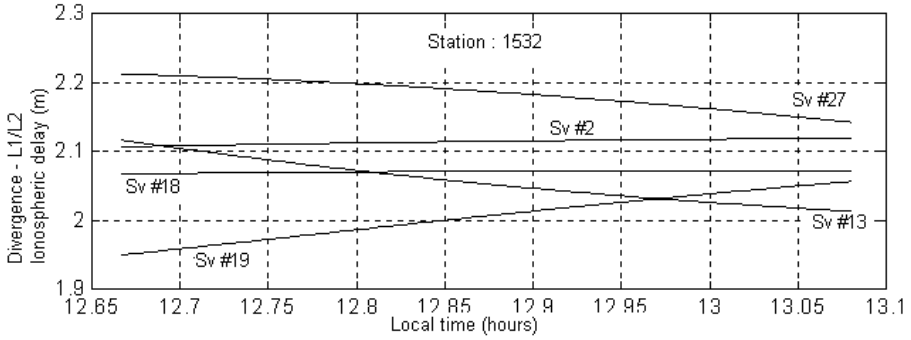

Fig.12. Differences between delays computed from divergence model and dual frequency solution at station 1532.

Table 1. *The statistics of the residuals of the carrier phase observations in the least-squares adjustments for satellite SV19.Units in metres*

Baseline	Maximum	Minimum	Standard Deviation	Average
JASK – 1637 (72 km)	0.100	-0.068	0.030	-0.005
1637 – 1532 (15 km)	0.006	-0.012	0.005	-0.003

Table 2. *Errors before and after applying the four-parameter model.*

Baseline	Error in longitude(m)		Error in Latitude(m)		Error in height(m)		Phase ambiguity		Relative error on baseline (ppm)	
	Before model	After model	Before model	After model	Before model	After model	Before model	After model	Before model	After model
JASK – 1637 (72 km)	0.093	0.018	0.060	0.029	0.035	0.020	Not fixed	fixed	0.37	0.15
1637 – 1532(15 km)	0.006	0.003	0.039	0.020	0.034	0.016	fixed	fixed	0.96	0.89

Table 3. *Errors before and after applying the divergence model.*

Baseline	Error in longitude(m)		Error in Latitude(m)		Error in height(m)		Phase ambiguity		Relative error on baseline (ppm)	
	Before	After	Before	After	Before	After	Before	After	Before	After
JASK – 1637 (72 km)	0.093	0.032	0.060	0.041	0.035	0.018	Not fixed	Fixed	0.37	0.22
1637 – 1532 (15 km)	0.006	0.011	0.039	0.031	0.034	0.048	Fixed	Fixed	0.96	1.27